Driving strategy for minimal energy consumption of an ultra-energy-efficient vehicle in Shell Eco-marathon competition

Driving strategy for minimal energy consumption of an ultra-energy-efficient vehicle in Shell Eco-marathon competition

Tsvetomir Gechev[1] and Plamen Punov

Department of combustion engines, automobiles and transport, Technical University of Sofia, 8, Kl. Ohridski blvd., 1756, Sofia, Bulgaria

[1] E-mail: tsv.gechev@gmail.com

Abstract. The paper focuses on the different driving strategies (driving cycles) for minimisation of the energy consumption of an ultra-energy-efficient electric vehicle developed by students for Shell Eco-marathon competition. The vehicle runs on hydrogen fuel and completes a set track with a 1420 m length and zero vertical deviation which is used for the 2019 European edition of the contest. A dynamic simulation model of the vehicle is developed taking into account vehicle resistance forces. A simplified model of the propulsion system is also described and used in the simulation. The propulsion system consists of a hydrogen fuel cell with a 1 kW rated power output, electric motors, electric converters, motor controllers and transmission. Furthermore, a strategy overview is proposed by which the vehicle complies with all necessary strategy limitations deriving from the competition rules. The various driving strategies, that comply with the competition average speed and differ from one another by the number of motors and transmission ratio, are simulated. The optimisation is done by changing the maximal and the minimal no-load speeds of the vehicle. A comparison of the energy usage is therefore conducted based on these strategies and the optimal one is chosen. In conclusion, additional driving strategies are proposed, in case more vehicle manoeuvrability or simpler driving style are desired during the race.

1. Introduction

The road transport sector produces around a fifth of the annual greenhouse gases (GHG) in Europe and is primarily responsible for the bad air quality in cities [1]. Unlike other sectors of the economy, transport has not experienced a gradual decline of the emissions and in the overall energy consumption in recent years [2]. Europe is not only a big consumer of vehicles, but also a big producer, with about 6.1% of the working people in EU being employed in the sector [3]. Furthermore, G. Fontaras revealed in his profound study [4], that the official laboratory emission values in Europe, more notably the ones of CO_2, are significantly lower than the values obtained from the actual on-road vehicle performance. Having all this in mind, the European Commission has developed a new low-emission mobility strategy, aiming at making transportation less polluting and safer, not only by bettering the efficiency of the newly produced vehicles from the contemporary vehicle fleet (the 2020-21 reference CO_2 emission target for new cars is 95 g per km [5]), but also by deploying vehicles with zero on-board GHG emissions [1, 6].

Hydrogen represents a serious pretender to replace the fossil fuels, as the hydrogen-based renewable energy production in Europe has gradually increased and is directly dependant on economic growth [7]. Particularly in the automotive applications, hydrogen is used in fuel cell electric vehicles (FCEVs) where it is transformed into electricity by the fuel cell (FC), whose only other products are heat and water [8].

Among the various types of FCs, the Proton Exchange Membrane (PEM) FC has proven to be the most suitable choice for such applications, being highly efficient [9, 10]. The frequent starts and stops, the sudden changes and the widely varying power demand require from the fuel cell systems to fast adapt to the operating conditions. Such conditions could easily be coped up with if the fuel cell system is hybridised using an additional energy storage such as batteries and/or supercapacitors (SCs) [9, 10]. Moreover, this allows for the storage of regenerative energy, since the fuel cell alone could not handle the regenerative braking energy flux. Such systems are more robust as they also benefit the fuel economy and further improve the dynamic performance of the FC. In [11] Fathabadi proves their advantage by experimentally studying the performance of a FCHEV powered by 90 kW FC and 600 F SCs, which provided a 435 km range with 5.4 kg hydrogen consumption as the maximum vehicle speed was 158 kmh^{-1} and the vehicle weight – 1800 kg.

The various possible approaches to building a fuel cell system with an auxiliary energy storage were of an interest to many scientific researches. The architecture of the hybrid systems with the choice of energy management strategies and a road model cycle are of a particulate significance for the efficiency of the vehicle. In [12] for example, Marzougui et al. proposes an energy management algorithm for a FC hybrid vehicle with a battery and SCs as energy storage system, which aims at regulating the energy provided from all three electric sources. The algorithm is evaluated on New European Driving Cycle (NEDC) and the results confirm its effectiveness in terms of power demand and energy efficiency. In [13] Carignano proposes an energy management strategy for a light commercial vehicle, tested on the standard Manhattan Bus Cycle (MBC) and the Buenos Aires Bus Cycle (BABC), while [14] investigates the effectiveness of SCs hybrid electric propulsion system for the same vehicle type on NEDC and ECE-15 cycles. [15] proposes a methodology for sizing of the energy storage system validated for the Worldwide Harmonized Light Vehicle Test Cycle (WLTC), while Kaya in his work [16] examines two new control strategies of FCHEV on standard “stop-go” and “uphill” road models. In [17] a multiphysics model for driving strategy optimisation of an Urban Concept vehicle is proposed, which led to maximal performance of 500 Wh/100km with 25 kmh^{-1} average speed.

Most of the studies were conducted on standardised driving cycles with set acceleration curves at any time of the cycle. They also mostly estimated the energy management of light duty vehicles, where the advantages of a hybrid propulsion systems are obvious due to the large power fluctuation and the availability of regenerative braking. Very few, though, are the researches focusing on real the driving strategy (driving cycle), notably for ultra-energy-efficient vehicles, where there is a limited speed range with and a very low efficiency of regenerative braking.

Firstly, this study is focused on the driving strategy architecture for an ultra-energy-efficient vehicle, powered by a FC and SCs as an additional energy source, which operates on a set track and with a set average speed. Then it proposes the most suitable driving strategies for energy efficiency, vehicle manoeuvrability and driving feasibility on the same track, by optimising the maximal and minimal no-load speed of the vehicle, and the transmission ratio, while maintaining the constant average speed. The energy efficiency optimisation is calculated for the electric power output, without taking into account the necessary power output of the FC, its efficiency and the efficiency of the SCs.

2. Competition and vehicle overview

In Shell Eco-marathon school and university students establish teams in which they develop a vehicle from its initial stages of design up to the final stages of production and assembly. These vehicles are divided into two categories: Prototype and Urban Concept, as each of them aims at reaching the lowest possible energy consumption, yet fulfilling different design requirements – Prototypes are made as slick and drop-like as possible, minimising resisting forces and maximising energy efficiency, while Urban Concept vehicles are created more similar to the conventional vehicles. The vehicles in each category could be electric – using a battery or a fuel cell as an energy source, or with an internal combustion engine (ICE) – running on gasoline, diesel or CNG fuel.

The main target for the teams is to cover a certain distance for a set amount of time by using minimal energy/fuel. As of 2019, the main European competition has been held at Mercedes-Benz World track in London, Great Britain. The track is 1420 m long and has no change in the elevation profile. An official track completion is recorded only when the vehicle covers 11 complete laps (15 620 m) in less than 39 minutes, hence the average speed is about 25 kmh^{-1}. Each team is given four attempts at completing the track. In order to recreate operation in urban conditions, Urban Concept vehicles must stop at the finish line once per lap.

Technical University of Sofia has a twelve-year-old tradition of taking part in the Shell Eco-marathon competition. The latest car was built in 2019 to compete in the Urban Concept – hydrogen fuel cell category in the same year in London (see figure 1). The car is significantly lighter than its predecessors due to the utilisation of a fully carbon-fibre body. According to the competition rules, the maximum vehicle weight without the driver is 225 kg, while the driver should be at least 70 kg. Additionally, hydrogen powered vehicles could use only supercapacitors as an energy storage system. The energy which is stored in them at the finish line of each lap has to be at least as much as that at the starting line. This is controlled by altering the SCs voltage. Moreover, regenerative braking is not allowed, as it overcomplicates the propulsion system and is also less efficient when integrated in vehicles of such size.

Figure 1. Vehicle of TUS Team.

In addition, the realisation of a hybrid propulsion system with a fuel cell and SCs, as well as the possibility of overloading of the motors, is possible by utilisation of buck/boost DC/DC convertors. Figure 2 represents a simple schematic of the vehicle propulsion.

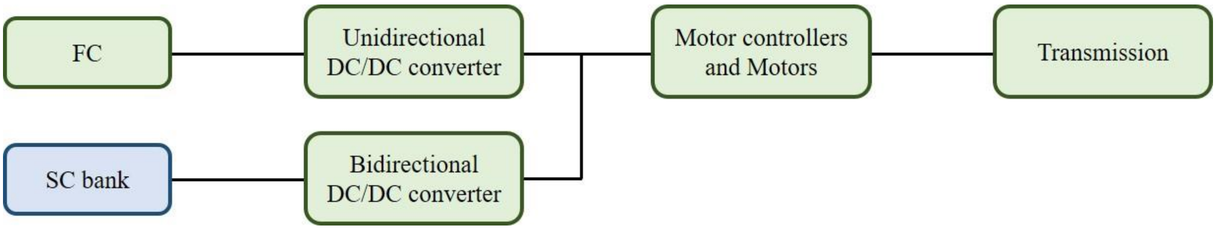

Figure 2. Car propulsion schematic.

3. Simulation model

3.1. Vehicle dynamic model

The power demand and energy consumption of the vehicle are calculated by means of a dynamic vehicle model. The force balance in longitudinal direction is given in (1), taking into account the traction force, rolling resistance, air resistance and inertia forces [8]. Due to the constant track profile, grade resistance is not included in the equation.

$$F_{tr} = F_i + F_{roll} + F_{aero}. \tag{1}$$

Therefore, the following equation (2) is used for estimating the instantaneous vehicle acceleration, where m is the vehicle mass and $\ddot{x}$ – its acceleration:

$$m\ddot{x} = F_{tr} - F_{roll} - F_{aero}. \tag{2}$$

The traction force is calculated in (3) by using the electric torque of the motor/motors M_{mot}, the transmission ratio (TR) i_{tr}, the transmission efficiency η_{tr}, and the dynamic radius of the wheel r_{roll}. The transmission efficiency is assumed constant as a single stage spur gear is used. The dynamic wheel radius is assumed equal to the static one, because of the low vehicle weight and the high tyre pressure.

$$F_{tr} = \frac{M_{mot} i_{tr} \eta_{tr}}{r_{roll}}. \tag{3}$$

The rolling and air resistances are calculated according to equations (4) and (5), where f_0 is rolling resistance coefficient at low speeds, k is an additional coefficient, ρ_a is air density, S_v is frontal area of the vehicle, c_x is drag flow coefficient and $\dot{x}$ – vehicle speed. In [11] the aerodynamic characteristics of this designed vehicle body were studied and the CFD results were then validated for a scaled model in a wind tunnel.

$$F_{roll} = mg(f_0 + k\dot{x}), \tag{4}$$

$$F_{aero} = \frac{1}{2}\rho_a S_v c_x \dot{x}^2. \tag{5}$$

The total mass of the vehicle and the inertial moments of all moving parts are calculated as a sum of the gross mass of the vehicle and the mass equivalent to the inertia moments, also taking into account the transmission ratio. The main parameters of the car are displayed in table 1, where Δm represents the reduced rotating masses.

Table 1. Main parameters of the vehicle.

Vehicle type	m_v, kg	Δm, kg	r_{roll}	f_0	k	S_v, m^2	C_x	η_{tr}	i_{tr}
Urban Concept	170	10.05	0.275	0.004	6.10^{-6}	0.795	0.136	0.95	200/12 or 200/13

3.2. *Traction motor and propulsion*

The motors used in our simulation are Maxon RE65, 36 V nominal voltage, 250 W nominal power, brushed DC with permanent magnets, that utilise coreless technology so that the hysteresis losses are minimised. The efficiency is about 90-91 % and the motors mostly function in overload mode due to their limited operation time during the race. The motor controllers have current limitation I_{mot} set at 9.5 A and the motors are overloaded by altering the input voltage U_{mot} up to 44-45 V. The maximum permitted motor voltage according to the competition rules is 48 V. By overloading the motors by voltage, the torque M_{mot} and angular velocity ω_{mot} are also increased above the nominal. Their correlation with the motor power P_{mot} is given in (6).

$$P_{mot} = \frac{M_{mot} \pi n_{mot}}{30}. \tag{6}$$

The motor torque M_{mot} and friction losses M_f are calculated according to (7) and (8), as k_m is motor torque constant and I_0 is no load current constant:

$$M_{mot} = k_m I_{mot} - M_f, \tag{7}$$

$$M_f = k_m I_0. \tag{8}$$

Motor efficiency $\boldsymbol{\eta_{mot}}$ and electric power $\boldsymbol{P_{el}}$ are calculated as follows:

$$\eta_{mot} = \frac{\pi n_{mot}}{30} \frac{(M_{mot}+M_f)}{U_{mot} I_{mot}}, \tag{9}$$

$$P_{el} = \frac{P_{mot}}{\eta_{mot}}. \tag{10}$$

The angular velocity of the motor n_{mot} is estimated by the following equation, where k_n is speed motor constant and $\frac{\Delta n}{\Delta M}$ is speed/torque gradient.

$$n_{mot} = k_n U_{mot} - \frac{\Delta n}{\Delta M} M_{mot}. \tag{11}$$

The motor controller ESCON 70/10 is used for motor management, due its high flexibility of control, most notably the possibility of closed loop current control, angular position control and speed control. In our simulation the torque of the motor is controlled by changing of its current I_{mot}, which is dependant on the level to which the acceleration pedal of the vehicle is engaged. A 100 % pushed acceleration pedal represents $I_{mot} = 9.3$ A. The main parameters and constants of the motor are shown in table 2, where P_N, U_N, I_N, M_N and n_N, are nominal values. The motor controller parameters are given in table 3, where U_{CC} is nominal operating voltage and I_{cont} is continuous output current.

Table 2. Main parameters of the electric motor.

Type	P_N, W	U_N, V	I_N, A	M_N, Nm	n_N, rpm	k_n, rpmV^{-1}	k_m, NmA^{-1}	I_0, A	η_{max}
DC RE 65	250	36	9.32	751.10^{-3}	3700	113	84.4.10^{-3}	0.6	0.87

Table 3. Main parameters of the motor controller.

Type	P_{max}, W	U_{cc}, V	I_{cont}, A	I_{max}, A	η_{max}
ESCON 70/10	700	10-70	10	30 (< 20 s)	98 %

3.3. Simulation limitations and strategy overview

3.3.1. Simulation limitations

In the process of generating different driving strategies and comparing their energy efficiency it is important to set proper simulation limitations so that the results are realistic and the strategies are not only feasible, but also fulfilling the rules of the competition. The main conditions defining the simulation are:

- Completion of 11 laps, S=1420 m each (total 15 620 m) within 39 mins, therefore an average speed of at around 25 kmh^{-1} for the whole strategy (cycle), maximal strategy length amounting to 210 s and $V_{start} = 0$ and $V_{finish} = 0$, in order to simulate operation in urban conditions (see figure 3);
- Maximal vehicle deceleration of 1 ms^{-2} during braking until stop at the end of each lap;
- Maximal operating voltage and current through the electric motors of the vehicle: U_{mot}^{max}= 44 V, I_{mot}^{max} = 9.3 A. I_{mot}^{max} is achieved in overload mode and should not be operated at for long periods of time;
- Only non-regenerative braking used;

- Maximum acceleration used in all acceleration periods of the vehicle, I_{mot}^{max} = 9.3 A = 100 % acceleration pedal push.

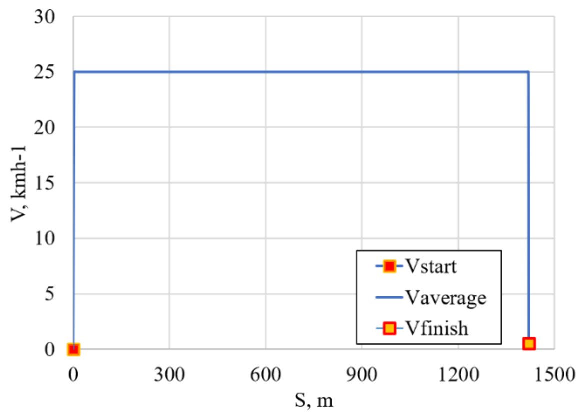

Figure 3. Main simulation limitations.

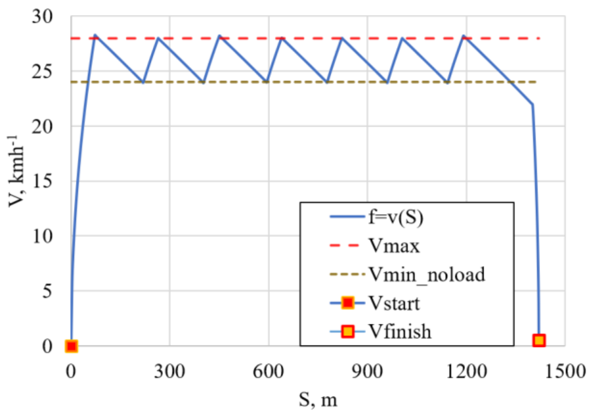

Figure 4. Proposed standard driving strategy.

3.3.2. Strategy overview

In ideal conditions the vehicle would not meet any traffic and would not have to undertake any unscheduled manoeuvres such as sudden acceleration or braking. Additionally, the power area from figure 3 could take any form and at the same time comply with the simulation limitations. Therefore, a standard driving strategy is proposed (see figure 4), consisting of the following parts:

- initial acceleration phase (IAP) from $V_{start} = 0$ up to V_{max},
- followed by an acceleration-coasting field (ACF) – plateau, in which the vehicle accelerates to V_{max}, then coasts down to the minimal speed at no-load V_{min}^{nl} and then again accelerates to the maximum speed, thus maintaining a slightly higher average speed in ACF than the one set for the whole strategy,
- followed by the last phase before the finish line which could contain either just braking, or braking and coasting to the minimal speed at the end of the strategy $V_{finish} = 0$.

In order to further define the strategy, it is important to examine each of the above-mentioned phases separately.

The vehicle could realise IAP with either 1 or 2 electric motors with the same transmission ratio. According to calculations, in terms of fulfilling the main limitations of the simulation, it is significantly better for the vehicle to accelerate with 2 motors during this period (see figure 5).

This way, not only does the vehicle reach V_{max} and ACF more quickly, while complying with the time limitation and even leaving a time reserve, but it also has an overall higher efficiency (see figure 6), by reaching more quickly the area in which the electric motors maintain their highest efficiency (the area is at high motor angular velocities – it matches with the plateau), and so lowering the energy consumption of the whole driving strategy. Therefore, IAP is realised via 2 traction motors.

ACF is where the most of the actual simulation and energy consumption comparison takes place. The optimisation is accomplished by varying certain parameters – the maximal speed V_{max}, minimal no-load speed V_{min}^{nl} and the number of motors used in the process of accelerating between the two speeds (see figure 7).

The last driving strategy period could be realised either by long and intensive braking due to the relatively high vehicle speed just before the finish line, or by a certain long coasting period after the last acceleration in ACF, followed by shorter braking. According to the calculations, the overall energy consumption of the driving strategy is better when starting to coast earlier and use braking just before the finish line, since this long coasting period at the end of each lap enables the usage of the accumulated kinetic energy during ACF (see figure 8). Moreover, it also represents a large compensative time reserve used during the whole driving strategy in cases of unexpected manoeuvres, sudden accelerations or decelerations, which are absolutely certain as the conditions during the racing are not ideal.

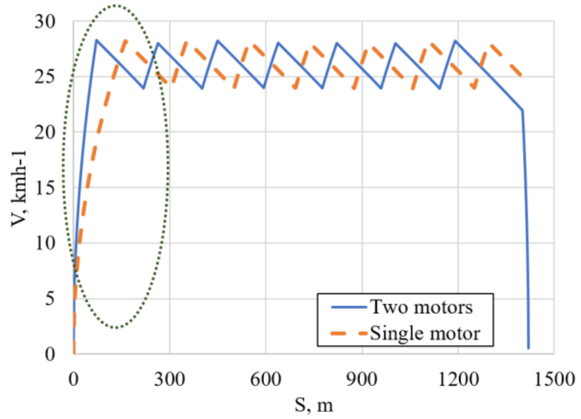

Figure 5. Comparison of IAP when using 1 or 2 traction motors (the bubble indicates IAP).

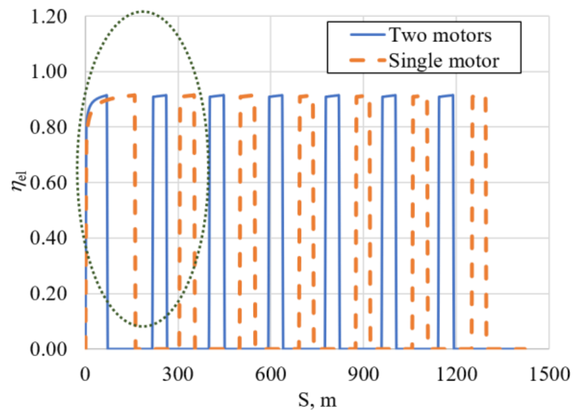

Figure 6. Comparison motor efficiency during IAP when using 1 or 2 traction motors (the bubble indicates IAP).

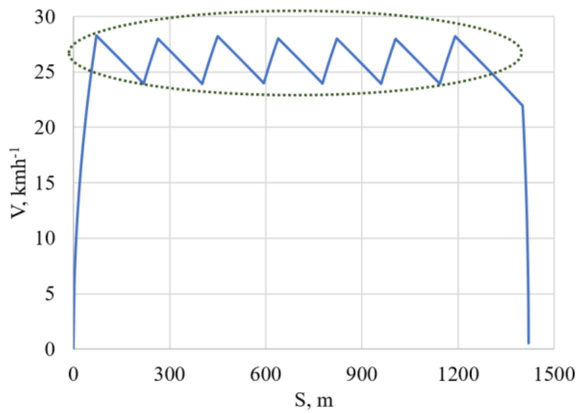

Figure 7. ACF representation – the bubble.

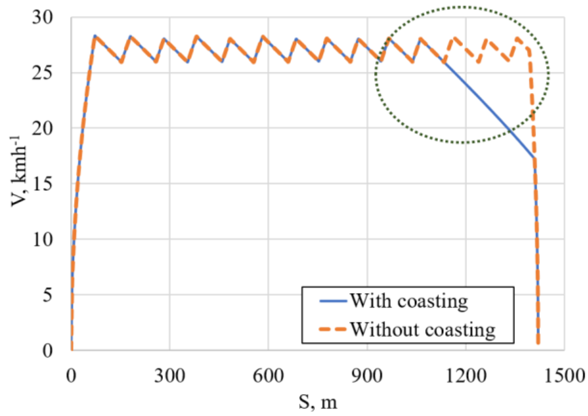

Figure 8. Using only braking in the final phase compared to using braking and coasting (the bubble indicates the final phase).

Once having the defining conditions set, the driving strategies are obtained by changing a few optimisation parameters. A total of 36 different strategies were studied in which the number of traction motors (excluding IAP), the transmission ratio (during the whole driving strategy) and the maximal V_{max} and minimal no-load V_{min}^{nl} speeds, were varied (see table 4).

4. Simulation results

In table 4 are given the case results of all 36 studied cases, that include all varying parameters, as well as the total electric motor cumulative energy used till the end of the driving strategy for each lap. All driving strategies have the set geometry of the proposed standard driving strategy (see figure 4) with a two traction motors IAP, followed by ACF and a final phase of long coasting and braking, as the cycle finishes for 210 s. In the column “comparative energy consumption” is given the energy consumption in percentage of each selected cycle compared to the one of the first one (case 1 – 100 %). In green colour are marked the results showing the lowest energy consumption.

Table 4. Results.

Case No	Motor Nominal Voltage, V	TR	Number of motors	Maximal speed, kmh^{-1}	Minimal no-load speed, kmh^{-1}	Used cumulative energy, J	Comparative energy consumption, %
1	36	200/12 =16.6	1	28	24	20920.00	100.00
2					25	20611.49	98.53
3					26	19556.57	93.48
4				29	25	19706.81	94.20
5					26	19547.83	93.44
6					27	19389.91	92.69
7				30	26	19391.86	92.70
8					27	19235.17	91.95
9					28	19225.87	91.90
10	36	200/12 =16.6	2	28	24	20913.55	99.97
11					25	20006.36	95.63
12					26	19691.54	94.13
13				29	25	19702.18	94.18
14					26	19391.23	92.69
15					27	19378.68	92.63
16				30	26	19386.15	92.67
17					27	19235.63	91.95
18					28	19224.69	91.90
19	36	200/13 =15.4	1	28	24	21347.32	102.04
20					25	20369.08	97.37
21					26	19942.95	95.33
22				29	25	19943.73	95.33
23					26	19795.36	94.62
24					27	19509.68	93.26
25				30	26	19649.53	93.93
26					27	19501.72	93.22
27					28	19355.47	92.52
28	36	200/13 =15.4	2	28	24	20787.57	99.37
29					25	20222.56	96.67
30					26	19930.35	95.27
31				29	25	19938.94	95.31
32					26	19650.86	93.93
33					27	19508.04	93.25
34				30	26	19514.17	93.28
35					27	19505.13	93.24
36					28	19346.02	92.48

On the basis of the results, the following conclusions are made:

- The optimisation in terms of TR shows that the lower TR – 200/13, leads to higher energy consumption due to the slower acceleration periods and slower reaching of the high efficiency zone of the motors, compared to TR 200/12 (see figure 9 – comparison of cases 1 and 19, 2% higher energy consumption). Despite of this, the TR 200/13 has also a few advantages – the motors operate in lower velocities, thus experiencing less stress from overloading and there is also a compensative speed reserve for possible acceleration over V_{max}.

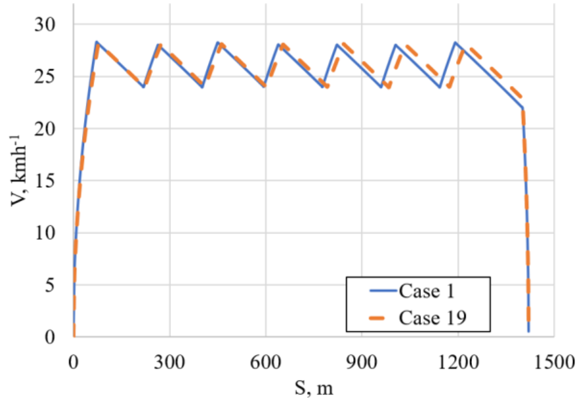

Figure 9. Comparison of cases 1 and 19, with respectively 200/12 and 200/13 TR.

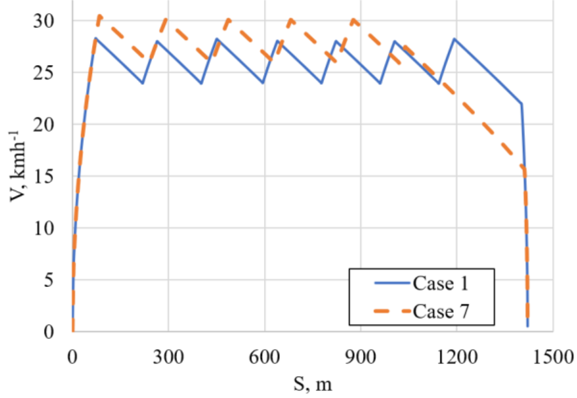

Figure 10. Comparison of cases 1 and 7, having different average speed during ACF.

- A higher average speed during the ACF – plateau, for strategies with both a single or two traction motors and all TR, leads to lower energy consumption. Additionally, a higher set V_{max} also ensures accumulation of the needed kinetic energy significantly earlier, this way also resulting in a longer coasting phase at the end of the cycle (see figure 10 – a comparison of cases 1 and 7, 7.3 % lower energy consumption). On the other hand, if the set maximal speed is too high, there is no speed reserve over V_{max}, due to technical limitations of the electric motors – U_{mot}^{max}= 44 V, I_{mot}^{max} = 9.3 A, and it also puts more stress on the motor/motors during overload mode. In real conditions it is very likely for the vehicle to need to accelerate over the set V_{max}, in order to compensate for lost time during unexpected manoeuvres.
- A smaller range between V_{max} and V_{min}^{nl} speeds and thus a higher average speed in the plateau results in less energy consumption for both a single and two traction motor strategies and all TR, yet there are more frequent accelerations during ACF, which could make it more difficult to implement the strategy by the pilot in real conditions (see figure 11– comparison of cycles case 1 and case 3, around 6.50 % lower energy consumption).
- Acceleration during the whole cycle by means of two traction motors results in approximately the same (or slightly lower) energy consumption. The advantages of such a strategy are in the higher manoeuvrability, due to the faster accelerations, and also in the more favourable conditions for the electric motors that work less time in overload regimes (see figure 12 – comparison between cases 1 and 10). Such a strategy, though, is less feasible in real conditions because of its higher ACF complexity – there are on average 1 to 2 more accelerations in ACF when the strategy adopts 2 traction motors in comparison to its 1 traction motor counterpart.

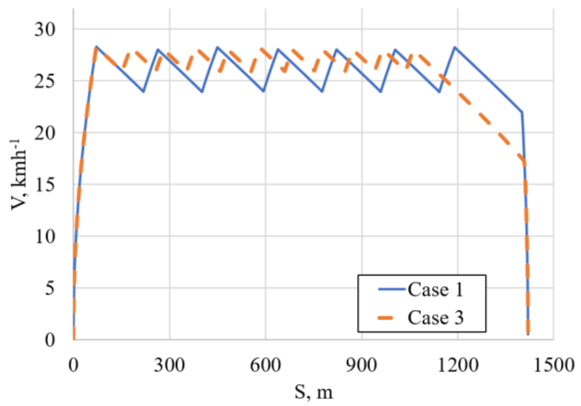

Figure 11. Comparison of cases 1 and 3, having different range between V_{max} and V_{min}^{nl} .

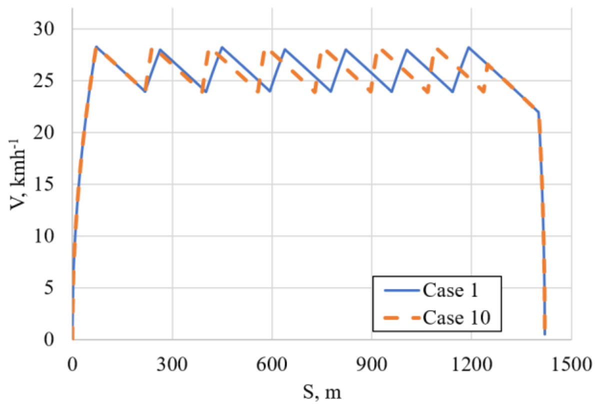

Figure 12. Comparison of cases 1 and 10, with respectively 1 and 2 traction motors.

5. Conclusions

Overall, there are many different options when choosing the correct driving strategy of an ultra-energy-efficient vehicle for this particular track in the competition. There is a well-established tendency of lowering of the energy consumption as the average plateau speed increases (up to 8 % difference in the energy consumption). Strategies with TR 200/13 consume more energy compared to these with TR 200/12, yet they offer better speed reserves over the maximal speed, and also maintain less overloading of motors during operation. Utilisation of two traction motors during acceleration in the whole cycle guarantees more manoeuvrability of the vehicle, yet such strategies become more complex to perform in real driving conditions.

When having to choose the right strategy, in terms of greater manoeuvrability, a less energy efficient strategy with lower V_{max}, two motors and TR 200/13, is suitable (see table 4, case 32, which consumes 19650.86 J of energy or is approximately 2.2 % less energy efficient than the most efficient strategy). If a lower level of complexity, yet higher efficiency is desired, a single motor, TR 200/12 and a large V_{max} - V_{min}^{nl} range, is chosen (see table 4, case 7, consuming 19391.86 J or around 0.8 % more energy than the most efficient strategy). Given that the desired cycle should purely be the most efficient one, a complex, two traction motor, with high average speed and a 200/12 TR strategy is chosen (see table 4, case 18 – consuming 19224.69 J).

Acknowledgements
This work was supported by the Bulgarian Ministry of Education and Science under the National Research Program "Low-carbon energy for transport and domestic use" approved by DCM # 577/17.08.2018.

References

[1] European Commission 2016 A European Strategy for low-emission mobility *Transp. Emiss* COM (2016) 501. https://ec.europa.eu/clima/policies/transport_en Accessed on 14.07.2020
[2] European Energy Agency 2015 Final energy consumption by sector and fuel *Indic. Assess. Data maps* ENER 016 (2020) https://www.eea.europa.eu/data-and-maps/indicators/final-energy-consumption-by-sector-10/assessment Accessed on 14.07.2020
[3] European Commission 2019 Internal Market, Industry, Entrepreneurship and SMEs *Eur. Comm.* https://ec.europa.eu/growth/sectors/automotive/ Accessed on 14.07.2020
[4] Fontaras G, Zacharof N G and Ciuffo B 2017 Fuel consumption and CO_2 emissions from passenger cars in Europe – Laboratory versus real-world emissions *Prog. Energy Combust. Sci.* **60** pp 97–131
[5] Parliament E U and E 2019 *Reducing CO2 emissions from passenger cars* Regulation (EC) No

443 (2009) https://ec.europa.eu/clima/policies/transport/vehicles/cars_en Accessed on 14.07.2020

[6] Pasaoglu G, Honselaar M and Thiel C 2012 Potential vehicle fleet CO_2 reductions and cost implications for various vehicle technology deployment scenarios in Europe *Energy Policy* **40** pp 404–21

[7] Xu R, Chou L C and Zhang W H 2019 The effect of CO_2 emissions and economic performance on hydrogen-based renewable production in 35 European Countries *Int. J. Hydrogen Energy* **44**(56) pp 29418–25

[8] Ehsani M, Gao Y and Emadi A 2017 *Modern Electric, Hybrid Electric, and Fuel Cell Vehicles* (CRC Press) p 348, p 22

[9] Wang Y, Chen K S, Mishler J, Cho S C and Adroher X C 2011 A review of polymer electrolyte membrane fuel cells: Technology, applications, and needs on fundamental research *Appl. Energy* **88**(4) pp 981–1007

[10] Bendjedia B, Rizoug N, Boukhnifer M and Bouchafaa F 2017 Hybrid Fuel Cell/Battery Source Sizing and Energy Management for Automotive Applications *IFAC-PapersOnLine* **50**(1) pp 4745–50

[11] Fathabadi H 2018 Fuel cell hybrid electric vehicle (FCHEV): Novel fuel cell/SC hybrid power generation system *Energy Convers. Manag.* **156** pp 192–201

[12] Marzougui H, Amari M, Kadri A, Bacha F and Ghouili J 2017 Energy management of fuel cell/battery/ultracapacitor in electrical hybrid vehicle *Int. J. Hydrogen Energy* **42** pp 8857–69

[13] Carignano M G, Costa-Castelló R, Roda V, Nigro N M, Junco S and Feroldi D 2017 Energy management strategy for fuel cell-supercapacitor hybrid vehicles based on prediction of energy demand *J. Power Sources* **360** pp 419–33

[14] Veneri O, Capasso C and Patalano S 2018 Experimental investigation into the effectiveness of a super-capacitor based hybrid energy storage system for urban commercial vehicles *Appl. Energy* **227** pp 312–23

[15] Gaikwad S D and Ghosh P C 2020 Sizing of a fuel cell electric vehicle: A pinch analysis-based approach *Int. J. Hydrogen Energy* **45**(15) pp 8985–93

[16] Kaya K and Hames Y 2019 Two new control strategies: For hydrogen fuel saving and extend the life cycle in the hydrogen fuel cell vehicles *Int. J. Hydrogen Energy* **44** pp 18967–80

[17] Olivier J-C, Wasselynck G, Chevalier S, Auvity B, Josset C, Trichet D, Squadrito G and Bernard N 2017 Multiphysics modeling and optimization of the driving strategy of a light duty fuel cell vehicle *Int. J. Hydrogen Energy* **42** pp 26943–55

[18] Dobrev I, Massouh F, Danlos A, Todorov M and Punov P 2017 Experimental and numerical study of the flow field around a small car *MATEC Web Conf.* **133** 02004